Tetrahedron 66 (2010) 8304–8312

Contents lists available at ScienceDirect

Tetrahedron

journal homepage: www.elsevier.com/locate/tet

Synthesis and liquid crystalline behavior of azulene-based liquid crystals with 6-hexadecyl substituents on each azulene ring

Kosuke Nakagawa [a], Takahiro Yokoyama [a], Kozo Toyota [a], Noboru Morita [a], Shunji Ito [b,*], Shota Tahata [b], Mao Ueda [b], Jun Kawakami [b], Miho Yokoyama [c], Yoriko Kanai [c], Kazuchika Ohta [c]

[a] Department of Chemistry, Graduate School of Science, Tohoku University, Sendai 980-8578, Japan
[b] Graduate School of Science and Technology, Hirosaki University, Hirosaki 036-8561, Japan
[c] Smart Materials Science and Technology, Department of Bioscience and Textile Technology, Interdisciplinary Graduate School of Science and Technology, Shinshu University, Ueda 386-8567, Japan

ARTICLE INFO

Article history:
Received 4 June 2010
Received in revised form 30 July 2010
Accepted 5 August 2010
Available online 12 August 2010

Keywords:
Discotic liquid crystals
Homeotropic alignment
Azulenes
Cyclotrimerization

ABSTRACT

Hexakis(6-hexadecyl-2-azulenyl)benzene (**1b**) has been synthesized by $Co_2(CO)_8$-catalyzed cyclotrimerization reaction of bis(6-hexadecyl-2-azulenyl)acetylene (**2b**). The mesomorphic behaviors of **1b**, **2b**, and 6-hexadecyl-2-phenylazulene (**3b**) were studied by differential scanning calorimetry (DSC), polarizing optical microscopy (POM), and X-ray diffraction (XRD) techniques and their mesomorphic properties were compared with those of their 6-octyl derivatives **1a**, **2a**, and **3a**. Increase of the number of carbon atoms in the peripheral side chains drops the isotropization temperatures of **1b**, **2b**, and **3b** by 56.9 °C, 33 °C, and 23.6 °C, respectively. Additionally, the phase-transition behavior varied with increase of the number of the peripheral chains, as well as decrease of the crystalline–mesophase transition temperatures, except for compound **3b**. As the results, spontaneous monodomain homeotropic molecular alignment was revealed by compound **1b** in its Col_{hd} mesophase on non-treated glass substrate, which would be attracted to the application for the device fabrication of molecular materials.

1. Introduction

Spontaneous or controllable alignment of molecules on a substrate is an important factor for device fabrication of molecular materials.[1] Disk-like compounds with long alkyl chains have attracted interest because of their ability to self-assemble to form columnar mesophases.[2] The stacking behavior of the disk-like compounds as discotic liquid crystals (LCs) provides opportunities for materials with one-dimensional transport processes, such as energy migration, electric conductivity, and photoconductivity.[3] Some discotic liquid crystalline semiconductors are recently found to show very fast carrier mobility.[4] However, both defects and polydomain boundaries in the discotic LCs may prevent the charge carrier transport in the liquid crystalline phase. To obtain better functional performance requires appropriate large-area-uniformity for the application to the device fabrication.[5] Therefore, controlling the alignment of discotic mesophases becomes a crucial point for the molecular design of the discotic liquid crystalline semiconductors. However, the conventional techniques applied to nematic phase are not useful for the alignment control of highly ordered columnar LCs. For example, vibrational excitation is applied to the alignment control of the Col_h mesophase for 2,3,6,7,10,11-hexaalkoxytriphenylene derivatives to induce homeotropic orientation; i.e., discs flat-on to the surface or 'horizontal'.[6] However, discotic liquid crystalline materials have a chance to induce spontaneous homeotropic alignment without domain boundaries and disclinations by their modification. Indeed, by introduction of fluoroalkylated chains into the peripheral parts, triphenylene mesogens lead to get a strong tendency of the homeotropic alignment.[7] Nevertheless, discotic LCs exhibiting spontaneous homeotropic alignment without domain boundaries and disclinations are very exceptional.[8]

Azulene ($C_{10}H_8$) has attracted the interest of many research groups because of its unusual properties and its beautiful blue color.[9] Amphoteric redox properties of the azulene derivatives are especially attractive to construct advanced materials for electronic applications. However, to date, molecules with potentially useful electronic properties constructed from azulene derivatives are fairly scarce. Substituted azulene derivatives linked to nematogenic alkylcyclohexanes by an ester function have been reported in the literatures to show nematic or smectic mesomorphisms.[10] Recently, we have reported the synthesis of the first azulene derivatives exhibiting discotic liquid crystalline behaviors.[11] Novel hexakis(6-octyl-2-azulenyl)benzene (**1a**) surrounding six octyl groups exhibits the columnar mesophases, Col_{ho}, with unusually

* Corresponding author. Tel.: +81 172 39 3568; fax: +81 172 39 3541; e-mail address: itsnj@cc.hirosaki-u.ac.jp (S. Ito).

0040-4020/$ – see front matter © 2010 Published by Elsevier Ltd.
doi:10.1016/j.tet.2010.08.012

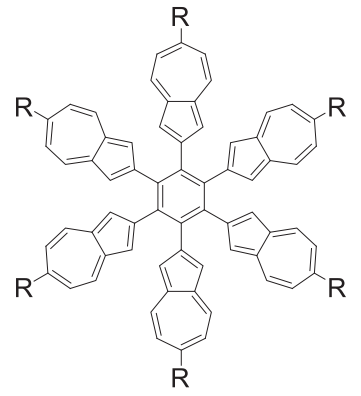

1a: R = C_8H_{17}
1b: R = $C_{16}H_{33}$

2a: R = C_8H_{17}
2b: R = $C_{16}H_{33}$

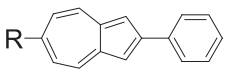

3a: R = C_8H_{17}
3b: R = $C_{16}H_{33}$

Figure 1. Azulene-based discotic liquid crystals.

large staking distances (h=5.20–5.52 Å) owing to the propeller conformation of the molecule (Fig. 1).[12]

The large size of the aromatic core of **1a** might have advantage for the preparation of the highly conductive materials, because the size of the aromatic core of the discogen may set the upper limit on the carrier mobility.[13] However, in general, the ordered functional materials constructed by large π-aromatic core would have high viscosity, which may induce domain boundaries in their columnar mesophases.[8] In spite of the large discogen core, compound **1a** may sustain fluidity in the LC mesophases owing to the large staking distances, which may reduce the interaction of the large π-aromatic core. Lower viscosity resulting from the sterically hindered aromatic core might induce the uniform alignment in the columnar mesophases. Therefore, we have investigated the introduction of longer alkyl chains to the hexakis(2-azulenyl)benzene core to increase the flexibility of the peripheral side chains, which induced a spontaneous perfect homeotropic alignment without domain boundaries and disclinations for the first time in azulene-based columnar LCs. Herein, we report the comparative study of the mesomorphic properties of hexakis(6-hexadecyl-2-azulenyl)benzene (**1b**), bis(6-hexadecyl-2-azulenyl)acetylene (**2b**), and 6-hexadecyl-2-phenylazulene (**3b**) with those of their 6-octyl derivatives **1a**, **2a**, and **3a**[12] to investigate the influence of the peripheral side chains in length (Fig. 1).

2. Results and discussion

2.1. Synthesis

Preparation of hexakis(6-hexadecyl-2-azulenyl)benzene (**1b**) surrounding by six hexadecyl groups was accomplished by $Co_2(CO)_8$-catalyzed cyclotrimerization reaction of bis(6-hexadecyl-2-azulenyl) acetylene (**2b**), as similar to the synthesis of **1a** by the reaction of 6,6′-dioctyl derivative **2a**.[12] Preparation of **1b** via **2b** commenced with diethyl 6-bromo-2-methoxyazulene-1,3-dicarboxylate (**4**);[12,14] it is outlined in Schemes 1–3. Pd-catalyzed cross-coupling reaction of **4** with 1-hexadecyne under Sonogashira–Hagihara conditions afforded diethyl 6-(1-hexadecynyl)-2-methoxyazulene-1,3-dicarboxylate (**5**) in almost quantitative yield. Catalytic hydrogenation of **5** utilizing Pd–C catalyst produced reduced compound **6** in 94% yield. After the two ester parts of **6** were hydrolyzed under basic conditions to give **7**, treatment of **7** with 100% H_3PO_4, which was freshly prepared by dissolving phosphorous pentaoxide in 85% phosphoric acid, afforded a mixture of 2-hydroxy and 2-methoxy derivatives **8** and **9** in 71% and 10% yields, respectively (Scheme 1).

The product **8** was transformed into 2-bromo derivative **10** by the treatment with PBr_3 in 80% yield. The Pd-catalyzed cross-coupling reaction of **10** with trimethylsilylacetylene at 60 °C afforded 6-hexadecynyl-2-(trimethylsilylethynyl)azulene (**11**) in 89% yield. Treatment of **11** with potassium fluoride in dimethylformamide (DMF) furnished 2-ethynyl-6-octylazulene (**12**) in 95% yield (Scheme 2).

Since the cross-coupling reaction of 2-ethynylazulene with 2-bromoazulene using $Pd(PPh_3)_4$ as a catalyst affords a mixture of di(2-azulenyl)acetylene and di(2-azulenyl)diacetylene, which may be produced by the Pd-catalyzed oxidative coupling of 2-ethynylazulene, the halogen exchange reaction of **10** was examined to give the desired 2-iodo derivative **13**. Although the halogen exchange reaction of **10** with a mixture of copper(I) iodide and potassium iodide in refluxing DMF should afford the desired **13** in 84% yield, we encountered with the difficulties in the reproducibility of this halogen exchange reaction (Scheme 2). The less effectiveness of the halogen exchange reaction might be attributed to insufficient solubility of **10** by increase the number of carbon atoms in the alkyl chain under these reaction conditions.

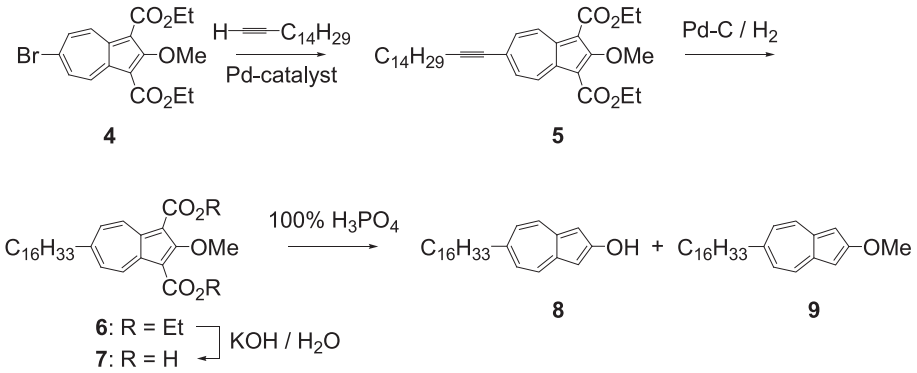

Scheme 1. Preparation of 6-hexadecyl-2-hydroxyazulene (**8**).

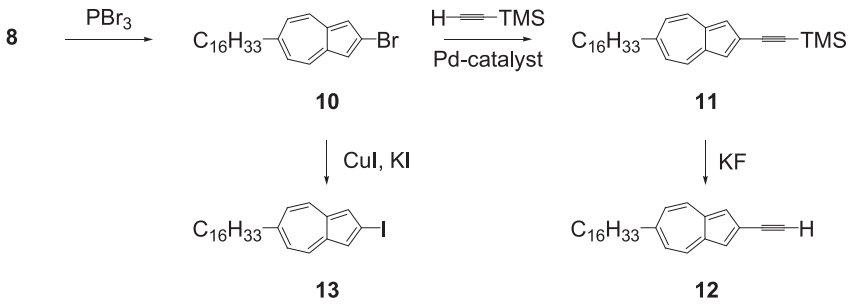

Scheme 2. Preparation of 2-ethynyl-6-hexadecylazulene (**12**) and 6-hexadecyl-2-iodoazulene (**13**).

Scheme 3. Preparation of hexakis(6-hexadecyl-2-azulenyl)benzene (**1b**).

However, the cross-coupling reaction of 6-alkyl-2-ethynyl derivative **12** readily proceeded with 2-bromo derivative **10** to give the expected bis(6-hexadecyl-2-azulenyl)acetylene (**2b**) in 77% yield under the ordinary reaction conditions. It is noteworthy that the cross-coupling reaction proceeds readily utilizing the bromide **10** to give the presumed cross-coupling product in high yield. As a matter of course, the Pd-catalyzed cross-coupling reaction of **12** with 2-iodo-6-hexadecylazulene (**13**) also afforded the expected bis (6-hexadecyl-2-azulenyl)acetylene (**2b**) in 86% yield. Cyclo-origomerization of **2b** catalyzed by $Co_2(CO)_8$ gave the desired benzene derivative **1b** with high solubility in 78% yield, as similar to that of 6,6′-dioctyl derivative **2a** (Scheme 3). For comparison of the phase-transition behavior, 6-hexadecyl-2-phenylazulene (**3b**) was also prepared by Pd-catalyzed Miyaura–Suzuki cross-coupling reaction of **10** with phenylboronic acid in 85% yield (Scheme 4). The spectral features of compounds **1b**, **2b**, and **3b** are in agreement with the structure of these compounds as summarized in the Experimental section.

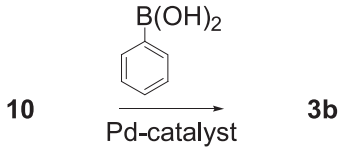

Scheme 4. Preparation of 6-hexadecyl-2-phenylazulene (**3b**).

Mass spectrum of compound **1b** measured by MALDI-TOF conditions showed correct $M+H^+$ ion peaks, which afford a criterion of the trimerized structure of compound **1b**. The absorption spectra of these compounds are quite similar with those of their 6-octyl derivatives **1a**, **2a**, and **3a**. They show the characteristic weak absorption of the azulene system in the visible region. The bathochromic shift of the longest absorption maxima of **1b** (λ_{max}=570 nm) in the visible region by 6 nm relative to that of **3b** (λ_{max}=564 nm) exhibits the extension of the π-system. The longest absorption maximum of **2b** (λ_{max}=569 nm) in the visible region exhibits a slight red shift (by 5 nm) compared with that of **3b** probably because of the electron-withdrawing nature of the substituted triple bond.[15]

2.2. Mesomorphic properties

Phase-transition behavior of **1b**, **2b**, and **3b** was examined with a polarizing microscope (POM) with a heating plate controlled by a thermoregulator and measured with a differential scanning calorimeter (DSC). The DSC thermograms of these compounds are shown in the Supplementary data. In Table 1, phase-transition temperatures and enthalpy changes determined by DSC for **1b**, **2b**, and **3b** are summarized. X-ray diffraction powder patterns were also measured with Cu Kα radiation to distinguish between the solid polymorphs in the compounds. The X-ray diffraction powder patterns of these compounds are shown in the Supplementary data. The assignments of X-ray reflections of each of the mesophases are summarized in Table 2. For the comparison, the phase-transition

Table 1
Phase-transition temperature (T) and enthalpy changes (ΔH) of compounds **1b**, **2b**, and **3b**[a]

Sample	Phase [b] $\xrightarrow[[\Delta H(\mathrm{kJ\ mol^{-1}})]]{T(^\circ\mathrm{C})}$ Phase
1b	$\mathrm{K(v)} \underset{[147]}{\overset{96.7}{\rightleftharpoons}} \mathrm{Col_{hd}} \underset{[6.80]}{\overset{143}{\rightleftharpoons}} \mathrm{I.L.}$
2b	$\mathrm{K_1(v)} \underset{[0.79]}{\overset{44.5}{\rightleftharpoons}} \mathrm{K_2} \underset{[1.07]}{\overset{59.2}{\rightleftharpoons}} \mathrm{K_3} \underset{[13.5]}{\overset{67.9}{\rightleftharpoons}} \mathrm{K_4} \underset{[7.32]}{\overset{85.2}{\rightleftharpoons}} \mathrm{K_5} \underset{[24.8]}{\overset{104}{\rightleftharpoons}} \mathrm{S_X} \underset{[1.13]}{\overset{148}{\rightleftharpoons}} \mathrm{S_C} \underset{[3.66]}{\overset{152}{\rightleftharpoons}} \mathrm{S_A} \underset{[12.1]}{\overset{182}{\rightleftharpoons}} \mathrm{I.L.}$
3b	$\mathrm{K(v)} \underset{[31.2]}{\overset{118}{\rightleftharpoons}} \mathrm{S_E} \underset{[19.7]}{\overset{157}{\rightleftharpoons}} \mathrm{I.L.}$

[a] Phase-transition temperature (T) and enthalpy change (ΔH) determined by DSC.
[b] Phase nomenclature: K=crystal; $\mathrm{Col_{hd}}$=hexagonal disordered columnar mesophase; $\mathrm{S_E}$=smectic E mesophase; $\mathrm{S_C}$=smectic C mesophase; $\mathrm{S_A}$=smectic A mesophase; $\mathrm{S_X}$=unidentified smectic mesophase; I.L.=isotropic liquid; (v)=fresh virgin state obtained by recrystallization from the solvent.

Table 2
X-ray diffraction data of the mesophase of compounds **1b**, **2b**, and **3b**

Sample	Mesophase Lattice constants/Å	Spacing/Å		Miller indices (hkl)
		Observed	Calculated	
1b	$\mathrm{Col_{hd}}$ at 122 °C	34.0	34.0	(100)
	a=39.2 Å	19.8	19.6	(110)
	Z=1.25 for ρ=1.00	17.1	17.0	(200)
	and h=3.40 Å[a]	13.0	12.8	(210)
		ca. 4.7	—	—[c]
2b	$\mathrm{S_A}$ at 167 °C	40.5	40.5	(001)
	c=40.5 Å	20.3	20.3	(002)
		13.5	13.5	(003)
		ca. 4.3	—	—[c]
	$\mathrm{S_C}$ at 150 °C	39.9	40.0	(001)
	c=40.0 Å	20.0	20.0	(002)
		13.4	13.3	(003)
		10.0	10.0	(004)
		ca. 4.4	—	—[c]
3b	$\mathrm{S_E}$ at 138 °C	33.4	33.4	(001)
	a=9.40 Å	16.9	16.7	(002)
	b=4.50 Å	11.3	11.1	(003)
	c=33.8 Å	8.50	8.35	(004)
	Z=2.01 for ρ=1.00[b]	4.70	4.70	(100)
		4.06	4.06	(110)
		3.32	3.25	(210)

[a] Number of molecules in a slice calculated by the assumption of the density of the mesophase (ρ=1.00 g cm^{-1}) and the average of the stacking distances (h=3.40 Å) in the $\mathrm{Col_{hd}}$ mesophase.
[b] Number of molecules in a 2D lattice calculated by the assumption of the density of the mesophase (ρ=1.00 g cm^{-1}).
[c] Halo of the molten alkyl chains.

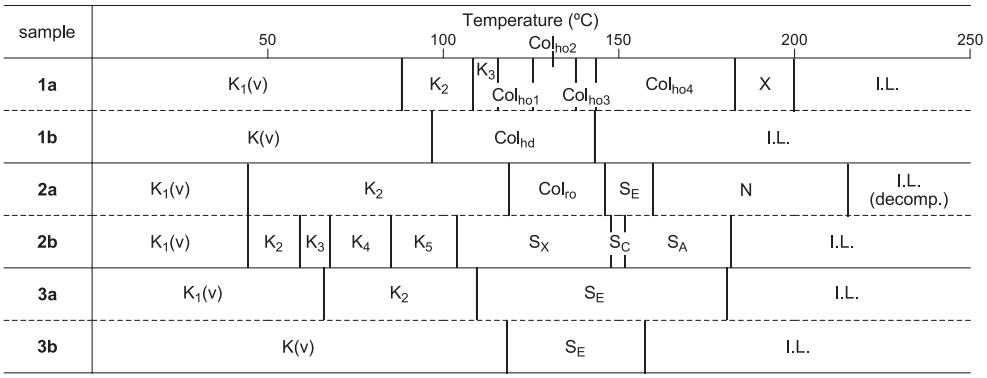

Figure 2. Graphical representation of the phase-transition temperatures of **1a**, **1b**, **2a**, **2b**, **3a**, and **3b**.

temperatures of **1b**, **2b**, and **3b** are represented schematically with those of 6-octyl derivatives **1a**, **2a**, and **3a** in Figure 2. The detailed thermal behaviors of these compounds are described below.

Compound **1b** showed mesomorphisms as summarized in Table 1. These state changes were observed in both the DSC measurements and the microscopic observations (Fig. 3). Recrystallization of **1b** from a solvent (CH_2Cl_2) at room temperature produced a crystalline phase, which was denoted as K(v) in Table 1. The K(v) crystals transformed into a mesophase at 96.7 °C, followed by an isotropic liquid (I.L.) at 143 °C. As expected, the isotropization temperature of compound **1b** drops by 56.9 °C with increasing the number of carbon atoms in the peripheral side chain. The crystalline–mesophase transition temperature is also decreased by 18.8 °C relative to that of 6-octyl derivative **1a** (115.5 °C). The phase transition enthalpy change was 147 kJ mol^{-1}, which is rather larger than that of a phase transition from a crystal to a columnar mesophase of 6-octyl derivative **1a** (21 kJ mol^{-1}). The enthalpy difference may have resulted from the length of the peripheral alkyl groups in these compounds. Therefore, the length of the mesogenic alkyl chains can markedly influence the phase-transition temperatures.

The X-ray diffraction experiments of the mesophase at 122 °C exhibited a diffuse band around 2θ=20° in the wide-angle region, which corresponds to the melt of the 6-hexadecyl chains. Compound **1b** also gave sharp four reflections corresponding to the spacing, 34.0, 19.8, 17.1, and 13.0 Å, in the small-angle region, which is characteristic of a Col$_h$ mesophase. However, the Col$_h$ mesophase did not give an additional reflection owing to the stacking distance (h) between disks in the column. Therefore, the phase was described as a disordered hexagonal columnar mesophase (Col$_{hd}$) in Table 2. The lattice constant (a) of the Col$_{hd}$ mesophase of compound **1b** became significantly longer than that of compound **1a** owing to the increase of the number of the carbon atoms in the peripheral side chain. The number of molecules (Z=1.25) in a slice presented in Table 2 was calculated by assuming the stacking distance h=3.40 Å (typical van der Waals radius of aromatic compounds) and the density ρ=1.00 g cm^{-3}. The Z value for compound **1b** is comparable with the usual number (Z=1) for the Col$_h$ mesophase. Therefore, the face-to-face stacking in the Col$_{hd}$ mesophase could be concluded to be much more attractive compared with that of the 6-octyl derivative **1a**. The reason may be attributed to the strong intermolecular interaction of the peripheral 6-hexadecyl substituents, which may induce the aggregation of the aromatic core to reduce the face-to-face stacking distance (h) of compound **1b** for the Col$_{hd}$ mesophase. Rather short stacking distance of compound **1b** in the Col$_{hd}$ mesophase should be attributable to the decreasing of the tilt angle of the 2-azulenyl groups.

When the isotropic liquid transformed into the Col$_{hd}$ mesophase, spontaneous homeotropic alignment could be observed on the non-treated glass plates, in which the development of a completely dark area between crossed polarizers (Fig. 3a). Upon holding at this temperature, the perfect homeotropic alignment grew within a minute as represented in Figures 3b and c. This is the first example to exhibit 'spontaneous uniform homeotropic alignment' in a discotic liquid crystalline azulene derivatives, so far as we know. The molecular difference between **1a** and **1b** consists only of the length of the alkyl chains in the surrounding. Therefore, it may be concluded that the longer alkyl chains induce the strong intermolecular interaction of the flexible large π-aromatic core to decrease the stacking distance and perfect homeotropic alignment on the non-treated glass substrate in these examples.

As expected, the 6-hexadecyl derivative **2b** also lowered isotropization temperature and varied with the mesomorphic behaviors. As can be seen from Table 1, compound **2b** exhibited mesomorphisms with crystalline polymorphs as similar with those of compound **2a**. Crystalline phase of **2b** obtained by recrystallization (hexane) was denoted as K$_1$(v) in Table 1. When the virgin crystals, K$_1$(v), were heated from room temperature, they exhibited subsequent solid–solid transitions at 44.5, 59.2, 67.9, and 85.2 °C to give the K$_2$, K$_3$, K$_4$, and K$_5$ crystals, respectively. On further heating, the K$_5$ crystals melted into a mesophase at 104 °C (ΔH=24.8 kJ mol^{-1}). As expected, the crystalline–mesophase transition temperature was also decreased by 14.8 °C relative to that of 6-octyl derivative **2a** (118.8 °C). The X-ray diffraction experiments of the mesophase at 126 °C exhibited reflections in the small-angle region characteristic for a smectic mesophase. The mosaic texture at 126 °C (Fig. 4d) should consist with a smectic mesophase, such as a smectic E (S$_E$) or a smectic B (S$_B$) mesophase. However, the X-ray diffraction experiments of the mesophase did not afford characteristic reflections such as S$_E$ mesophase in the wide-angle region around 2θ=20°. Therefore, the X-ray diffraction patterns did not allow us to unequivocal analysis of the lowest-temperature state, which was denoted as S$_X$ in Table 1.

Upon further heating, the unidentified S$_X$ mesophase transformed into a smectic C (S$_C$) mesophase at 148 °C (ΔH=1.13 kJ mol^{-1}) followed by a smectic A (S$_A$) mesophase at 152 °C (ΔH=3.66 kJ mol^{-1}). Generally, the enthalpy changes could not be observed at the S$_C$–S$_A$ phase transition. However, in some cases, it is also reported the small enthalpy changes at the S$_C$–S$_A$ phase transition.[16] The S$_C$–S$_A$ phase transition of **2b** exhibits rather large enthalpy change in the DSC measurements. The enthalpy changes of fusion depend on the length of the chains. The rather large enthalpy change at the S$_C$–S$_A$ phase transition of **2b** might be attributed to the two long C-16 alkyl chains substituted. Upon further heating, the S$_A$ mesophase clears to an I.L. at 182 °C. The crystalline–mesophase transition and isotropization temperatures of compound **2b** (cf. **2a**, 118.8 °C and 215.0 °C, respectively) dropped by 14.8 °C and 33 °C, respectively, with increasing the number of carbon atoms in the peripheral side chains. On the cooling

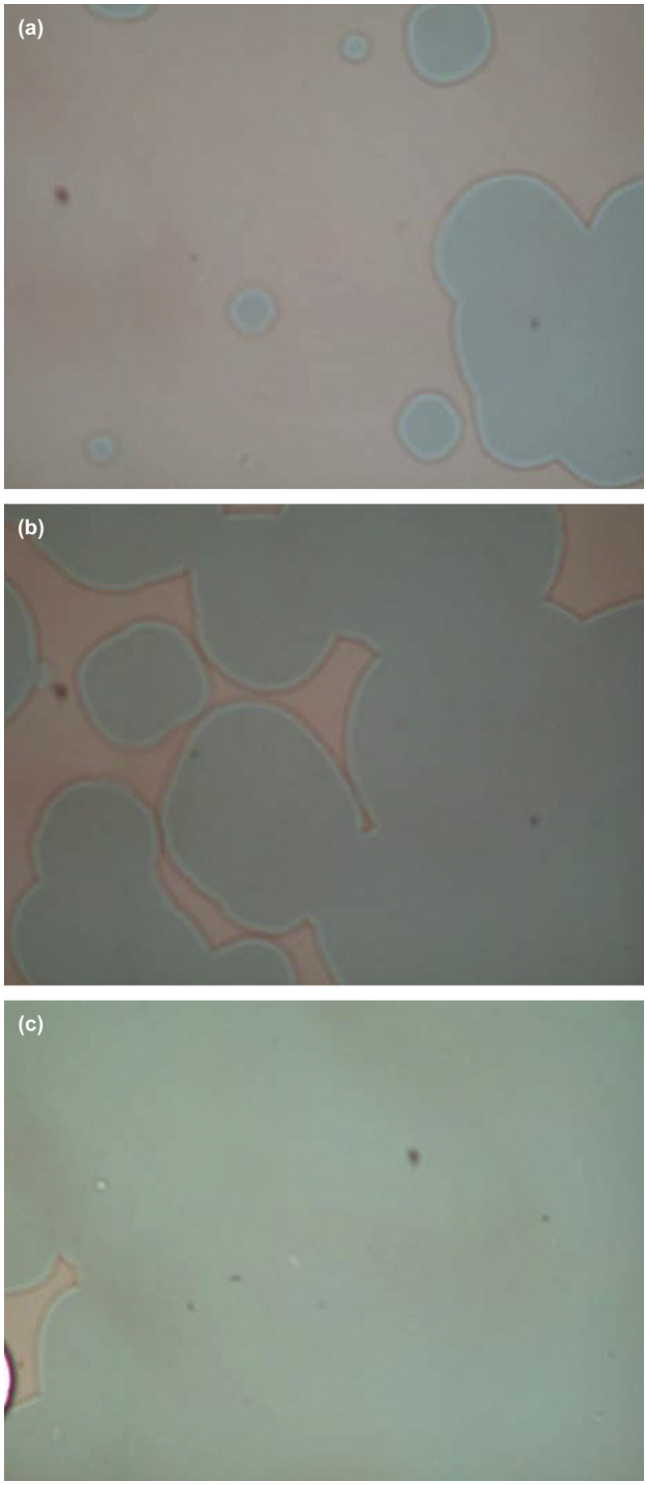

Figure 3. Microscopy images of the mesophase of compound **1b**; (a) Textures of compound **1b** obtained by cooling from the isotropic liquid at 135.5 °C; (b) Textures of compound **1b** obtained by standing at 135.5 °C; (c) Textures of compound **1b** obtained by further standing at 135.5 °C.

process from the I.L. phase, the development of batonnets was first observed at 167 °C. The appearance of the batonnets (Fig. 4a) should correspond to a smectic mesophase of compound **2b**. The batonnets coalesced and built up fan-shaped texture of the S_A mesophase (Fig. 4b) by standing the sample at that temperature, where the X-ray diffraction showed a typical pattern for smectic mesophase of c=40.5 Å. Compound **2b** had schlieren texture for the S_C mesophase (Fig. 4c), where the X-ray diffraction showed

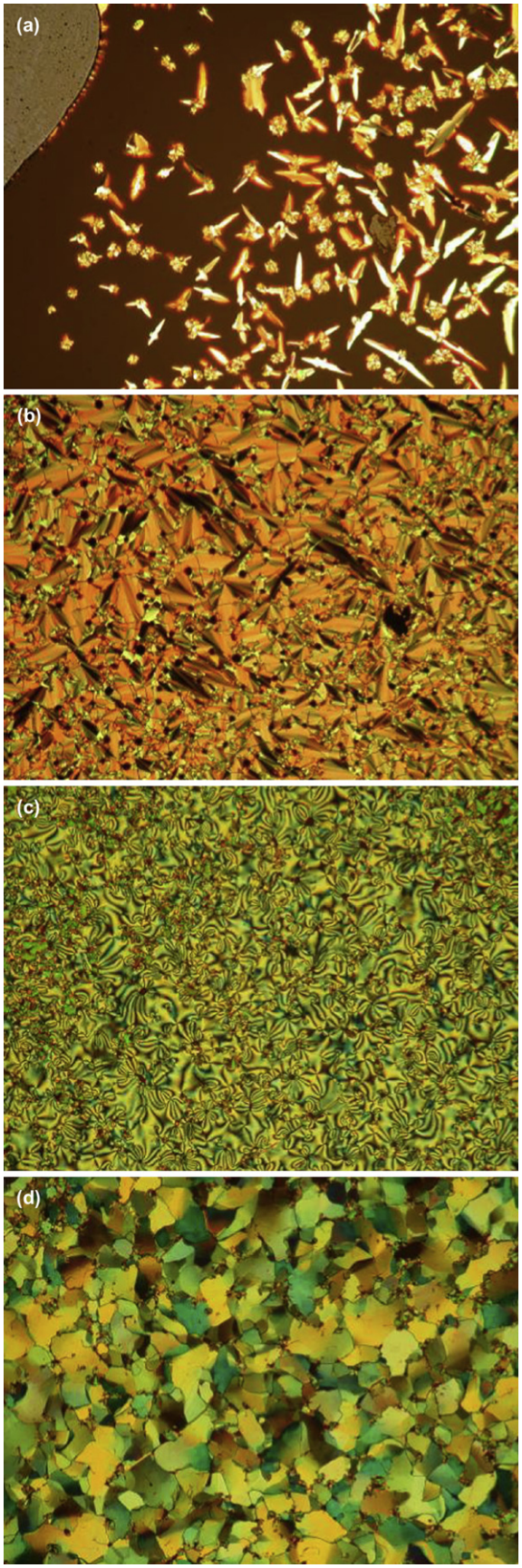

Figure 4. Textures of the mesophase of compound **2b**; (a) Batonnets observed at first by cooling from the isotropic liquid at 167 °C; (b) Fan-shaped texture of the S_A mesophase obtained when the sample stood at 167 °C; (c) Schlieren texture of the S_C mesophase at 150 °C; (d) Mosaic texture of the S_X mesophase at 126 °C.

a typical pattern for smectic mesophase of c=40.0 Å. The schlieren texture gives the unequivocal evidence of the S_C mesophase of **2b**.

Compound **3b** exhibited smectic mesomorphism as similar to that of compound **3a** (Table 1). Upon heating the sample, the K(v) crystals obtained by recrystallization of **3b** (hexane) transformed into the S_E mesophase at 118 °C (ΔH=31.2 kJ mol^{-1}). Upon further heating, the S_E mesophase cleared to an isotropic liquid (I.L.) at 157 °C (ΔH=19.7 kJ mol^{-1}). On the cooling process from the I.L. phase, compound **3b** developed grandjean terrace texture characteristic for the S_E mesophase (Fig. 5). The X-ray diffraction pattern of the mesophase at 138 °C showed a typical pattern for the S_E structure (Table 2). It showed two narrow reflections in the small-angle region which correspond to the (001) and (002) planes; the interlayer distance of 33.8 Å. It also had three reflections in the wide-angle region which correspond to (100), (110), and (210) in a two-dimensional rectangular lattice (lattice constants a=9.40 Å and b=4.50 Å). By assuming a specific gravity of 1.00 g cm^{-3}, we can estimate the average number of molecules per unit cell to be 2.01 molecules with the interlayer distance of 33.8 Å. The reflections arisen from the two-dimensional rectangular lattice, the average number of molecules per unit cell, and also the grandjean terrace texture at the mesophase represent the evidence of the S_E mesophase of **3b**.

Figure 5. Grandjean terrace texture of the S_E mesophase of compound **3b** obtained by cooling from the isotropic liquid at 153 °C.

The isotropization temperature of compound **3b** (cf. **3a**, 180.6 °C) dropped by 23.6 °C with increasing the number of carbon atoms in the alkyl chain as similar to those of **1b** and **2b**. However, the crystalline–mesophase transition temperature was increased by 8.4 °C relative to that of 6-octyl derivative **3a** (109.6 °C). Thus, the temperature range of the S_E mesophase becomes narrow with increasing the number of carbon atoms in the alkyl chain.

3. Conclusions

Hexakis(6-hexadecyl-2-azulenyl)benzene (**1b**) was successfully synthesized by $Co_2(CO)_8$-catalyzed cyclotrimerization reaction of **2b**. The mesomorphic behaviors of **1b**, **2b**, and **3b** have been clarified and were compared with those of 6-octyl derivatives **1a**, **2a**, and **3a**. Introduction of 6-hexadecyl chains as the peripheral tails provided a spontaneous perfect homeotropic alignment of a Col_{hd} mesophase in **1b** on the non-treated glass substrate. Therefore, the chain length is very important for the alignment controls of the discotic mesophases in these cases.

In general, the surface affinity of the molecules is modified by changing the chemical nature of the aromatic core or side chains. The examples of homeotropic alignment are of triphenylenes and phthalocyanines bearing heteroatoms in the side chains, which imply a strong influence of the substituents on the arrangement of the molecules. The long, flexible, hydrophobic alkyl chains are believed to force the system to minimize contact with polar substrates such as non-treated glass, which results in an 'edge-on' alignment of the molecules.[17] However, successful perfect homeotropic alignment of all-hydrocarbon compound **1b** should open a novel molecular design for the alignment controls of the discotic mesophases.

The homeotropic alignment is significant to increase the mobility of discotic LCs for practical usage such as photovoltaic diodes.[18] According to the Col_{hd} mesophase of compound **1b** easily self-organizes in columns perpendicular to the substrate when cooled from the isotropic liquid phase. Therefore, the present compound **1b** might exhibit excellent paths for charge carrier transportation and may become an intrinsic candidate for the future applications to a semiconductor owing the amphoteric redox properties of azulene derivatives.

4. Experimental section

4.1. General

Melting points were determined on a Yanagimoto micro melting apparatus MP-S3 and are uncorrected. Mass spectra were obtained with a Hitachi M-2500 or a Bruker APEX II instrument. IR and UV spectra were measured on a Shimadzu FTIR-8100M and a Hitachi U-3410 spectrophotometers, respectively. ^{1}H NMR spectra (^{13}C NMR spectra) were recorded on a JEOL GSX 400 spectrometer at 400 MHz (100 MHz). Gel permeation chromatography (GPC) purification was performed on a BIO-RAD Bio-Beads® S-X3 with CH_2Cl_2 as an eluent. Elemental analyses were performed at the Research and Analytical Center for Giant Molecules, Graduate School of Science, Tohoku University.

*4.1.1. Diethyl 6-(1-hexadecynyl)-2-methoxyazulene-1,3-dicarboxylate (**5**).* To a degassed solution of diethyl 6-bromo-2-methoxyazulene-1,3-dicarboxylate (**4**) (5.01 g, 13.1 mmol), 1-hexadecyne (5.85 g, 26.3 mmol), CuI (250 mg, 1.31 mmol), triethylamine (27 mL) in dry toluene (200 mL) was added tetrakis(triphenylphosphine)palladium(0) [$Pd(PPh_3)_4$] (765 mg, 0.662 mmol). The resulting mixture was stirred at room temperature for 1 h under an Ar atmosphere. The reaction mixture was washed successively with a 5% NH_4Cl solution and brine, dried over $MgSO_4$, and concentrated under reduced pressure. The residue was purified by column chromatography on silica gel with 20% ethyl acetate/hexane to afford **5** (6.79 g, 99%). Purple needles; mp 57.2–57.7 °C (MeOH); ^{1}H NMR (400 MHz, $CDCl_3$): δ=9.31 (d, $^3J_{H,H}$=11.3 Hz, 2H, 4,8-H), 7.73 (d, $^3J_{H,H}$=11.3 Hz, 2H, 5,7-H), 4.46 (q, $^3J_{H,H}$=7.1 Hz, 4H, 1,3-CO_2Et), 4.14 (s, 3H, 2-OMe), 2.49 (t, $^3J_{H,H}$=7.2 Hz, 2H, 3′-H), 1.65 (tt, $^3J_{H,H}$=7.2, 7.2 Hz, 2H, 4′-H), 1.46 (t, $^3J_{H,H}$=7.1 Hz, 6H, 1,3-CO_2Et), 1.40–1.20 (m, 22H, 5′–15′-H), 0.88 (t, $^3J_{H,H}$=6.8 Hz, 3H, 16′-H); ^{13}C NMR (100 MHz, $CDCl_3$): δ=170.27, 164.61, 141.45, 134.80, 134.67, 133.93, 108.07, 96.48, 84.30, 62.96, 60.19, 31.88, 29.65, 29.63, 29.49, 29.32, 29.10, 28.97, 28.43, 22.65, 19.73, 14.42, 14.07; IR (KBr disk): ν_{max}=2990 (w), 2982 (w), 2921 (s), 2851 (s), 2226 (w, C≡C), 1688 (w), 1678 (s, C=O), 1580 (w), 1566 (w), 1541 (w), 1487 (s), 1474 (w), 1429 (s), 1389 (s), 1331 (w), 1287 (s), 1246 (m), 1225 (m), 1200 (s), 1125 (w), 1111 (w), 1069 (w), 1038 (m), 999 (m), 880 (w), 860 (w), 797 (w), 789 (w), 720 (w), 710 (w), 695 (w), 604 (w), 567 (w), 534 (w), 480 (w), 430 (w) cm^{-1}; UV–vis (CH_2Cl_2): λ_{max} (log ε)=238 (4.43), 271 sh (4.17), 329 (4.92), 372 (4.24), 395 sh (3.89), 493 (2.73) nm; HRMS (ESI positive): calcd for $C_{33}H_{45}O_5$+Na^+ 545.3237; found 545.3237. Anal. Calcd for $C_{33}H_{46}O_5$: C, 75.83; H, 8.87; found: C, 75.63; H, 8.72.

*4.1.2. Diethyl 6-hexadecyl-2-methoxyazulene-1,3-dicarboxylate (**6**).* A mixture of diethyl 6-(1-hexadecynyl)-2-methoxyazulene-1,3-dicarboxylate (**5**) (3.58 g, 6.85 mmol) and 10% Pd–C (384 mg) in ethanol (74 mL) and THF (44 mL) was stirred at room temperature

for 6 h under an H_2 atmosphere. After the Pd catalyst was removed by filtration, the solvent was removed under reduced pressure. The residue was purified by column chromatography on silica gel with 10% ethyl acetate/hexane to afford **6** (3.40 g, 94%). Orange crystals; mp 56.1–56.3 °C (MeOH); ^{1}H NMR (400 MHz, $CDCl_3$): δ=9.41 (d, $^3J_{H,H}$=10.8 Hz, 2H, 4,8-H), 7.58 (d, $^3J_{H,H}$=10.8 Hz, 2H, 5,7-H), 4.46 (q, $^3J_{H,H}$=7.2 Hz, 4H, 1,3-CO_2Et), 4.13 (s, 3H, 2-OMe), 2.88 (t, $^3J_{H,H}$=7.6 Hz, 2H, 1′-H), 1.72 (tt, $^3J_{H,H}$=7.6, 7.6 Hz, 2H, 2′-H), 1.46 (t, $^3J_{H,H}$=7.2 Hz, 6H, 1,3-CO_2Et), 1.33–1.22 (m, 26H, 3′–15′-H), 0.87 (t, $^3J_{H,H}$=7.0 Hz, 3H, 16′-H); ^{13}C NMR (100 MHz, $CDCl_3$): δ=169.79, 164.83, 155.46, 140.89, 136.13, 132.29, 107.37, 62.96, 60.05, 41.71, 32.56, 31.90, 29.67, 29.63, 29.60, 29.50, 29.44, 29.33, 29.20, 22.67, 14.47, 14.09; IR (KBr disk): ν_{max}=2979 (w), 2953 (w), 2919 (s), 2853 (m), 1682 (s, C=O), 1582 (w), 1545 (w), 1495 (s), 1474 (m), 1460 (w), 1431 (s), 1416 (m), 1393 (m), 1377 (w), 1339 (w), 1300 (w), 1285 (m), 1279 (m), 1242 (m), 1231 (w), 1204 (m), 1154 (w), 1111 (w), 1084 (w), 1038 (m), 1032 (m), 1001 (m), 924 (w), 903 (w), 841 (w), 814 (w), 789 (w), 733 (w), 716 (w), 569 (w) cm^{-1}; UV–vis (CH_2Cl_2): λ_{max} (log ε)=270 (4.36), 314 (4.81), 348 (3.98), 370 sh (3.79), 463 (2.75) nm; HRMS (ESI positive): calcd for $C_{33}H_{50}O_5$+Na^+ 549.3550; found 549.3548. Anal. Calcd for $C_{33}H_{50}O_5$: C, 75.25; H, 9.57; found: C, 75.18; H, 9.57.

*4.1.3. 6-Hexadecyl-2-hydroxyazulene (**8**) and 6-hexadecyl-2-methoxyazulene (**9**).* Diethyl 6-hexadecyl-2-methoxyazulene-1,3-dicarboxylate (**6**) (2.80 g, 5.32 mmol) was dissolved in a solution of KOH (17.4 g, 0.310 mol) in water (70 mL) and ethanol (70 mL). The resulting mixture was refluxed for 4 h. After cooling the reaction mixture, water (500 mL) was added to the mixture and the combined mixture was acidified with 2 M HCl. The precipitated crystals were collected by filtration and dissolved in $CHCl_3$. The organic layer was dried over $MgSO_4$ and concentrated under reduced pressure to afford 6-hexadecyl-2-methoxyazulene-1,3-dicarboxylic diacid (**7**), which was utilized to the next reaction without further purification.

A mixture of **7** and freshly prepared 100% phosphoric acid (120 mL) was heated at 100 °C for 30 min with occasional stirring with a glass rod. After cooling the reaction mixture, the mixture was poured into ice-water (1.5 L) and extracted with toluene. The organic layer was washed with water, dried over $MgSO_4$, and concentrated under reduced pressure. The residue was purified by column chromatography on silica gel with 20% ethyl acetate/hexane to afford **8** (1.38 g, 71%) and **9** (203 mg, 10%).

Compound **8**: Reddish brown crystals; mp 88.0–88.5 °C (MeOH); ^{1}H NMR (400 MHz, acetone-d_6): δ=9.49 (s, 1H, 2-OH), 7.95 (d, $^3J_{H,H}$=10.4 Hz, 2H, 4,8-H), 7.11 (d, $^3J_{H,H}$=10.4 Hz, 2H, 5,7-H), 6.70 (s, 2H, 1,3-H), 2.77 (t, $^3J_{H,H}$=7.6 Hz, 2H, 1′-H), 1.70 (tt, $^3J_{H,H}$=7.6, 7.6 Hz, 2H, 2′-H), 1.39–1.25 (m, 26H, 3′–15′-H), 0.88 (t, $^3J_{H,H}$=7.0 Hz, 3H, 16′-H); ^{13}C NMR (100 MHz, acetone-d_6): δ=167.58, 148.09, 140.15, 131.12, 126.00, 103.77, 42.41, 33.71, 32.64, 30.37, 30.31, 30.07, 23.33, 14.35 (Several signals in aliphatic region could not be determined by overlapping with signals from acetone-d_6); IR (KBr disk): ν_{max}=2955 (w), 2917 (s), 2849 (s), 1657 (m), 1630 (w), 1580 (w), 1549 (m), 1538 (m), 1518 (m), 1472 (m), 1464 (m), 1437 (w), 1406 (w), 1366 (w), 1291 (w), 1262 (w), 1231 (w), 1169 (w), 1142 (w), 978 (w), 957 (w), 860 (w), 831 (m), 820 (w), 795 (w), 720 (w), 652 (w), 550 (w), 438 (w), 411 (w) cm^{-1}; UV–vis (CH_2Cl_2): λ_{max} (log ε)=281 (4.52), 290 (4.60), 322 sh (3.72), 362 sh (4.11), 373 (4.14), 393 sh (3.92), 444 sh (3.10), 474 sh (2.91), 516 sh (2.56) nm; HRMS (ESI positive) calcd for $C_{26}H_{40}O$+Na^+ 391.2971; found 391.2970. HRMS (ESI positive) calcd for $C_{26}H_{40}O$+H^+ 369.3152; found 369.3150. Anal. Calcd for $C_{26}H_{40}O$: C, 84.72; H, 10.94; found: C, 84.60; H, 10.65.

Compound **9**: Purple needles; mp 78.8–79.5 °C (hexane); ^{1}H NMR (400 MHz, $CDCl_3$): δ=7.99 (d, $^3J_{H,H}$=10.6 Hz, 2H, 4,8-H), 7.10 (d, $^3J_{H,H}$=10.6 Hz, 2H, 5,7-H), 6.76 (br s, 2H, 1,3-H), 4.02 (s, 2H, 2-OMe), 2.76 (t, $^3J_{H,H}$=7.6 Hz, 2H, 1′-H), 1.68 (tt, $^3J_{H,H}$=7.6, 7.6 Hz, 2H, 2′-H), 1.37–1.21 (m, 26H, 3′–15′-H), 0.88 (t, $^3J_{H,H}$=6.8 Hz, 3H, 16′-H); ^{13}C NMR (100 MHz, $CDCl_3$): δ=168.50, 148.53, 138.54, 131.46, 125.50, 100.95, 57.47, 42.00, 32.88, 31.93, 29.70, 29.67, 29.58, 29.54, 29.37, 29.33, 22.70, 14.11; IR (KBr disk): ν_{max}=3092 (w), 3015 (w), 2953 (w), 2917 (s), 2849 (s), 1584 (w), 1549 (m), 1526 (s), 1472 (m), 1464 (m), 1431 (m), 1410 (m), 1342 (w), 1293 (w), 1233 (w), 1204 (m), 1165 (w), 1144 (m), 1026 (m), 961 (w), 951 (w), 833 (m), 820 (w), 789 (w), 783 (m), 772 (w), 727 (w), 720 (w), 650 (w), 604 (w), 411 (w) cm^{-1}; UV–vis (CH_2Cl_2): λ_{max} (log ε)=283 (4.87), 292 (4.98), 320 (3.88), 344 (3.69), 360 (3.85), 376 (3.86), 510 (2.29), 540 sh (2.22), 589 sh (1.73) nm; HRMS (ESI positive): calcd for $C_{27}H_{42}O$+Na^+ 405.3128; found 405.3126. HRMS (ESI positive): calcd for $C_{27}H_{42}O$+H^+ 383.3308; found 383.3307. Anal. Calcd for $C_{27}H_{42}O$: C, 84.75; H, 11.06; found: C, 84.48; H, 11.15.

*4.1.4. 2-Bromo-6-hexadecylazulene (**10**).* To a solution of 6-hexadecyl-2-hydroxyazulene (**8**) (1.67 g, 4.53 mmol) in dry toluene (187 mL) was added PBr_3 (3.81 g, 14.1 mmol). The resulting mixture was heated at 90 °C for 50 min. The reaction mixture was poured into water (1.5 L) and extracted with toluene. The organic layer was washed with water, dried over $MgSO_4$, and concentrated under reduced pressure. The residue was purified by column chromatography on silica gel with hexane to afford **10** (1.56 g, 80%). Purple crystals; mp 82.8–83.2 °C (EtOH); ^{1}H NMR (400 MHz, $CDCl_3$): δ=8.13 (d, $^3J_{H,H}$=10.4 Hz, 2H, 4,8-H), 7.53 (s, 2H, 1,3-H), 7.12 (d, $^3J_{H,H}$=10.4 Hz, 2H, 5,7-H), 2.77 (t, $^3J_{H,H}$=7.6 Hz, 2H, 1′-H), 1.70 (tt, $^3J_{H,H}$=7.6, 7.6 Hz, 2H, 2′-H), 1.40–1.21 (m, 26H, 3′–15′-H), 0.88 (t, $^3J_{H,H}$=6.8 Hz, 3H, 16′-H); ^{13}C NMR (100 MHz, $CDCl_3$): δ=154.18, 138.55, 134.66, 125.76, 118.43, 42.43, 32.55, 31.93, 29.69, 29.66, 29.62, 29.53, 29.48, 29.36, 29.31, 22.69, 14.11; IR (KBr disk): ν_{max}=2951 (m), 2919 (s), 2851 (s), 2361 (w), 2342 (m), 1584 (w), 1545 (m), 1470 (w), 1441 (m), 1404 (w), 1235 (w), 1157 (w), 1073 (w), 974 (w), 916 (w), 862 (w), 839 (m), 791 (w), 768 (w), 720 (w), 691 (w), 669 (w), 596 (w), 440 (w) cm^{-1}; UV–vis (CH_2Cl_2): λ_{max} (log ε)=285 (4.90), 294 (4.89), 326 sh (3.65), 336 (3.79), 350 (3.85), 364 (3.86), 537 (2.65), 572 sh (2.60), 625 sh (2.18) nm; HRMS (ESI positive): calcd for $C_{26}H_{39}Br$+H^+ 431.2308; found 431.2346. Anal. Calcd for $C_{26}H_{39}Br$: C, 72.37; H, 9.11; found: C, 72.18; H, 9.21.

*4.1.5. 6-Hexadecyl-2-(trimethylsilyl)ethynylazulene (**11**).* Trimethylsilylacetylene (551 mg, 5.61 mmol) was added to a solution of 2-bromo-6-hexadecylazulene (**10**) (806 mg, 1.87 mmol), CuI (36 mg, 0.19 mmol), and tetrakis(triphenylphosphine)palladium(0) [$Pd(PPh_3)_4$] (108 mg, 0.0934 mmol) in triethylamine (9 mL) and dry toluene (47 mL). The resulting mixture was stirred at 60 °C for 30 min under an Ar atmosphere. The reaction mixture was poured into a 10% NH_4Cl solution and extracted with toluene. The organic layer was washed with brine, dried over $MgSO_4$, and concentrated under reduced pressure. The residue was purified by column chromatography on silica gel with hexane to afford **11** (747 mg, 89%). Blue crystals; mp 37.0–37.5 °C (EtOH); ^{1}H NMR (400 MHz, $CDCl_3$): δ=8.11 (d, $^3J_{H,H}$=10.3 Hz, 2H, 4,8-H), 7.34 (s, 2H, 1,3-H), 7.06 (d, $^3J_{H,H}$=10.3 Hz, 2H, 5,7-H), 2.76 (t, $^3J_{H,H}$=7.6 Hz, 2H, 1′-H), 1.69 (tt, $^3J_{H,H}$=7.6, 7.6 Hz, 2H, 2′-H), 1.40–1.21 (m, 26H, 3′–15′-H), 0.88 (t, $^3J_{H,H}$=7.0 Hz, 3H, 16′-H), 0.29 (s, 9H, TMS); ^{13}C NMR (100 MHz, $CDCl_3$): δ=154.72, 138.70, 136.19, 128.67, 125.16, 120.88, 103.36, 100.18, 42.49, 32.58, 31.92, 29.69, 29.66, 29.54, 29.49, 29.35, 22.68, 14.11, 0.04; IR (KBr disk): ν_{max}=2955 (m), 2917 (s), 2849 (s), 2147 (w), 1580 (m), 1485 (w), 1472 (m), 1455 (w), 1406 (m), 1375 (w), 1252 (m), 1015 (w), 972 (w), 901 (w), 857 (m), 837 (s), 808 (w), 758 (w), 729 (w), 718 (w), 698 (w), 668 (w), 646 (w), 436 (w), 409 (w) cm^{-1}; UV–vis (CH_2Cl_2): λ_{max} (log ε)=238 (4.14), 245 sh (4.08), 271 (4.38), 278 sh (4.37), 296 (4.80), 307 (4.88), 338 sh (3.60), 352 (3.78), 369 (4.13), 388 (4.33), 432 sh (1.64), 568 (2.61), 601 (2.61), 658 sh (2.26) nm; MS (70 eV): *m*/*z* (%)=448 (100) [M^+], 433 (6)

[M^+-CH_3], 377 (1) [M^+−TMS]. Anal. Calcd for $C_{31}H_{48}Si$: C, 82.96; H, 10.78; found: C, 82.94; H, 10.69.

*4.1.6. 2-Ethynyl-6-hexadecylazulene (**12**).* A solution of KF (195 mg, 3.36 mmol) in water (11 mL) was added to a solution of 6-hexadecyl-2-(trimethylsilyl)ethynylazulene (**11**) (747 mg, 1.66 mmol) in DMF (54 mL). After stirring the mixture at room temperature for 3 h, the reaction mixture was poured into water (500 mL) and extracted with toluene. The organic layer was washed with water, dried over $MgSO_4$, and concentrated under reduced pressure. The residue was purified by column chromatography on silica gel with hexane to afford **12** (598 mg, 95%). Blue crystals; mp 63.5–63.9 °C (EtOH); ^{1}H NMR (400 MHz, $CDCl_3$): δ=8.14 (d, $^3J_{H,H}$=10.4 Hz, 2H, 4,8-H), 7.37 (s, 2H, 1,3-H), 7.08 (d, $^3J_{H,H}$=10.4 Hz, 2H, 5,7-H), 3.43 (s, 1H, 2-C≡CH), 2.77 (t, $^3J_{H,H}$=7.6 Hz, 2H, 1′-H), 1.70 (tt, $^3J_{H,H}$=7.6, 7.6 Hz, 2H, 2′-H), 1.38–1.22 (m, 26H, 3′–15′-H), 0.88 (t, $^3J_{H,H}$=7.0 Hz, 3H, 16′-H); ^{13}C NMR (100 MHz, $CDCl_3$): δ=155.15, 138.60, 136.46, 127.57, 125.27, 120.88, 82.20, 82.05, 42.50, 32.56, 31.93, 29.69, 29.66, 29.54, 29.48, 29.35, 29.33, 22.69, 14.11; IR (KBr disk): ν_{max}=3316 (m), 2953 (w), 2919 (s), 2851 (s), 1580 (m), 1466 (m), 1410 (w), 1184 (w), 976 (w), 839 (m), 822 (w), 804 (w), 720 (w), 644 (w), 629 (m), 592 (m), 552 (w), 459 (w), 448 (w), 421 (w) cm^{-1}: UV–vis (CH_2Cl_2): λ_{max} (log ε)=238 (4.18), 268 (4.37), 292 (4.87), 303 (4.91), 333 sh (3.51), 348 (3.73), 362 (3.99), 370 sh (3.88), 380 (4.26), 568 (2.69), 602 (2.69), 660 sh (2.34) nm; MS (70 eV): *m*/*z* (%)=376 (100) [M^+], 347 (6) [$M^+-C_2H_5$], 333 (6) [$M^+-C_3H_7$], 319 (5) [$M^+-C_4H_9$], 305 (4) [$M^+-C_5H_{11}$]. Anal. Calcd for $C_{28}H_{40}$: C, 89.29; H, 10.71; found: C, 89.21; H, 10.84.

*4.1.7. 6-Hexadecyl-2-iodoazulene (**13**).* A solution of 2-bromo-6-hexadecylazulene (**10**) (1.07 g, 2.48 mmol), CuI (5.74 g, 30.1 mmol), KI (9.43 g, 56.8 mmol) in DMF (50 mL) was refluxed for 16 h. The reaction mixture was poured into water (300 mL) and extracted with toluene. The organic layer was washed with water, dried over $MgSO_4$, and concentrated under reduced pressure. The residue was purified by column chromatography on silica gel with hexane to afford **13** (995 mg, 84%). Purple plates; mp 88.8–89.2 °C (EtOH); ^{1}H NMR (400 MHz, $CDCl_3$): δ=8.14 (d, $^3J_{H,H}$=10.5 Hz, 2H, 4,8-H), 7.41 (s, 2H, 1,3-H), 7.10 (d, $^3J_{H,H}$=10.5 Hz, 2H, 5,7-H), 2.76 (t, $^3J_{H,H}$=7.6 Hz, 2H, 1′-H), 1.70 (tt, $^3J_{H,H}$=7.6, 7.6 Hz, 2H, 2′-H), 1.36–1.22 (m, 26H, 3′–15′-H), 0.88 (t, $^3J_{H,H}$=6.8 Hz, 3H, 16′-H); ^{13}C NMR (100 MHz, $CDCl_3$): δ=154.64, 139.24, 134.16, 125.51, 124.41, 96.38, 42.52, 32.49, 31.92, 29.68, 29.65, 29.52, 29.47, 29.35, 29.29, 22.68, 14.11; IR (KBr disk): ν_{max}=2951 (m), 2919 (s), 2851 (s), 1582 (m), 1466 (m), 1399 (m), 1233 (w), 974 (w), 912 (w), 839 (m), 820 (w), 791 (w), 720 (w), 615 (w), 590 (w) cm^{-1}; UV–vis (CH_2Cl_2): λ_{max} (log ε)=238 (4.12), 291 (4.83), 302 (4.90), 329 sh (3.63), 343 (3.79), 356 (3.85), 372 (4.01), 399 (2.46), 544 (2.65), 576 sh (2.61), 633 sh (2.18) nm; MS (70 eV): *m*/*z* (%)=478 (100) [M^+], 351 (18) [M^+−I]. Anal. Calcd for $C_{26}H_{39}I$: C, 65.26; H, 8.22; found: C, 65.26; H, 8.11.

*4.1.8. Bis(6-hexadecyl-2-azulenyl)acetylene (**2b**).* To a degassed solution of 2-ethynyl-6-hexadecylazulene (**12**) (400 mg, 1.06 mmol), 2-bromo-6-hexadecylazulene (**10**) (457 mg, 1.06 mmol), and CuI (23 mg, 0.12 mmol) in triethylamine (5 mL) and toluene (27 mL) was added tetrakis(triphenylphosphine)palladium(0) [$Pd(PPh_3)_4$] (63 mg, 0.054 mmol). The resulting mixture was stirred at 60 °C for 1.5 h under an Ar atmosphere. The reaction mixture was poured into a 10% NH_4Cl solution and extracted with toluene. The organic layer was washed with brine, dried over $MgSO_4$, and concentrated under reduced pressure. The residue was purified by recrystallization from hexane to afford **2b** (592 mg, 77%). Green plates; mp 184.5 °C (hexane); ^{1}H NMR (400 MHz, $CDCl_3$): δ=8.16 (d, $^3J_{H,H}$=10.4 Hz, 2H, 4,8-H), 7.46 (s, 2H, 1,3-H), 7.09 (d, $^3J_{H,H}$=10.4 Hz, 2H, 5,7-H), 2.78 (t, $^3J_{H,H}$=7.2 Hz, 2H, 1′-H), 1.71 (t, $^3J_{H,H}$=7.2 Hz, 2H, 2′-H), 1.41–1.20 (m, 26H, 3′–15′-H), 0.88 (t, $^3J_{H,H}$=6.8 Hz, 3H, 16′-H); ^{13}C NMR (100 MHz, $CDCl_3$): δ=154.49, 138.98, 135.95, 129.22, 125.25, 120.64, 93.86, 42.51, 32.60, 31.92, 29.69, 29.65, 29.55, 29.51, 29.36, 22.69, 14.11; IR (KBr disk): ν_{max}=2953 (w), 2917 (s), 2849 (s), 1578 (w), 1545 (w), 1471 (w), 1464 (w), 1410 (w), 837 (m), 720 (w), 642 (w), 417 (w) cm^{-1}; UV–vis (CH_2Cl_2): λ_{max} (log ε)=276 (4.58), 312 sh (4.96), 320 (5.05), 395 sh (4.50), 411 sh (4.68), 421 (4.75), 448 (4.92), 530 sh (3.03), 569 (3.13), 609 sh (3.07), 665 sh (2.67) nm; MS (70 eV): *m*/*z* (%)=727 (100) [M^+], 529 (3), 515 (3). Anal. Calcd for $C_{54}H_{78}\cdot 1/2H_2O$: C, 88.10; H, 10.82; found: C, 88.32; H, 10.72.

*4.1.9. Hexakis(6-hexadecyl-2-azulenyl)benzene (**1b**).* $Co_2(CO)_8$ (21 mg, 0.061 mmol) was added to a solution of bis(6-hexadecyl-2-azulenyl) acetylene (**2b**) (209 mg, 0.287 mmol) in 1,4-dioxane (73 mL). The mixture was refluxed for 20 h under an Ar atmosphere. After removing the solvent under reduced pressure, the residue was purified by column chromatography on silica gel with CH_2Cl_2 and Bio-Beads® S-X3 with CH_2Cl_2 to afford **1b** (164 mg, 78%). Green crystals; mp 141.0 °C (CH_2Cl_2); ^{1}H NMR (400 MHz, $CDCl_3$): δ=7.50 (d, $^3J_{H,H}$=10.4 Hz, 2H, 4,8-H), 6.62 (d, $^3J_{H,H}$=10.4 Hz, 2H, 5,7-H), 6.56 (s, 2H, 1,3-H), 2.57 (t, $^3J_{H,H}$=7.2 Hz, 2H, 1′-H), 1.57 (tt, $^3J_{H,H}$=7.2 Hz, 2H, 2′-H), 1.41–1.20 (m, 26H, 3′–15′-H), 0.88 (t, $^3J_{H,H}$=7.2 Hz, 3H, 16′-H); ^{13}C NMR (100 MHz, $CDCl_3$): δ=151.18, 149.85, 137.85, 137.74, 134.57, 122.93, 121.24, 42.27, 32.62, 31.93, 30.91, 29.71, 29.68, 29.60, 29.54, 29.50, 29.37, 22.69, 14.11; IR (KBr disk): ν_{max}=2919 (s), 2851 (s), 1576 (m), 1545 (w), 1508 (w), 1468 (m), 1414 (w), 1396 (m), 837 (m), 722 (w), 669 (w) cm^{-1}; UV–vis (CH_2Cl_2): λ_{max} (log ε)=288 (5.59), 317 sh (5.27), 384 sh (4.75), 570 (3.28), 608 sh (3.24), 671 sh (2.86) nm; MS (MALDI-TOF): *m*/*z* (%)=2180.8 (96) [M+H^+], 1865.4 (100) [$M^+-C_{23}H_{38}$]. Anal. Calcd for $C_{162}H_{234}$: C, 89.19; H, 10.81; found: C, 89.11; H, 10.66.

*4.1.10. 6-Hexadecyl-2-phenylazulene (**3b**).* A solution of 2-bromo-6-hexadecylazulene (**10**) (200 mg, 0.464 mmol), phenylboronic acid (114 mg, 0.935 mmol), Cs_2CO_3 (433 mg, 1.33 mmol), tetrakis(triphenylphosphine)palladium(0) [$Pd(PPh_3)_4$] (27 mg, 0.023 mmol) in dioxane (11 mL) was refluxed for 2 h under an Ar atmosphere. The reaction mixture was poured into water (200 mL) and extracted with CH_2Cl_2. The organic layer was washed with brine, dried over $MgSO_4$, and concentrated under reduced pressure. The residue was purified by column chromatography on silica gel with hexane to afford **3b** (169 mg, 85%). Blue plates; mp 154.1–154.5 °C (hexane); ^{1}H NMR (400 MHz, $CDCl_3$): δ=8.18 (d, $^3J_{H,H}$=10.4 Hz, 2H, 4,8-H), 7.94 (d, $^3J_{H,H}$=7.6 Hz, 2H, 2′,6′-H), 7.60 (s, 2H, 1,3-H), 7.45 (dd, $^3J_{H,H}$=7.6, 7.6 Hz, 2H, 3′,5′-H), 7.33 (t, $^3J_{H,H}$=7.6 Hz, 1H, 4′-H), 7.06 (d, $^3J_{H,H}$=10.4 Hz, 2H, 5,7-H), 2.77 (t, $^3J_{H,H}$=7.2 Hz, 2H, 1″-H), 1.71 (tt, $^3J_{H,H}$=7.2, 7.2 Hz, 2H, 2″-H), 1.41–1.20 (m, 26H, 3″–15″-H), 0.88 (t, $^3J_{H,H}$=7.2 Hz, 3H, 16″-H); ^{13}C NMR (100 MHz, $CDCl_3$): δ=153.10, 148.57, 139.93, 136.72, 135.41, 128.84, 127.87, 127.45, 124.97, 114.24, 42.39, 32.62, 31.92, 29.69, 29.65, 29.55, 29.51, 29.35, 22.68, 14.11; IR (KBr disk): ν_{max}=2951 (w), 2917 (s), 2849 (s), 1578 (m), 1549 (w), 1471 (m), 1441 (w), 1415 (w), 1026 (w), 908 (w), 837 (m), 756 (s), 720 (w), 687 (m), 450 (w) cm^{-1}; UV–vis (CH_2Cl_2): λ_{max} (log ε)=300 (4.90), 311 (4.96), 359 sh (3.92), 377 (4.22), 396 (4.29), 564 (2.63), 597 (2.61), 650 sh (2.25) nm; MS (70 eV): *m*/*z* (%)=428 (100) [M^+], 231 (11), 217 (15). Anal. Calcd for $C_{32}H_{44}$: C, 89.65; H, 10.35; found: C, 89.44; H, 10.23.

Acknowledgements

The present work was supported by the Ministry of Education, Culture, Sports, Science, and Technology, Japan by a Grant-in-Aid for Scientific Research (Grant 21550031 to S.I.).

Supplementary data

DSC thermograms of compounds **1b**, **2b**, and **3b**; X-ray diffraction powder patterns of compounds **1b**, **2b**, and **3b**. Supplementary data associated with this article can be found in online version at

doi:10.1016/j.tet.2010.08.012. These data include MOL files and InChIKeys of the most important compounds described in this article.

References and notes

1. See, e.g.: Wu, J.; Pisula, W.; Müllen, K. *Chem. Rev.* **2007**, *107*, 718–747.
2. (a) Chandrasekhar, S. *Liquid Crystals*, 2nd ed.; Cambridge University: Cambridge, 1992; (b) Bushby, R. J.; Lozman, O. R. *Curr. Opin. Colloid Interface Sci.* **2002**, *7*, 343–354.
3. (a) Adam, D.; Schuhmacher, P.; Simmerer, J.; Häussling, L.; Siemensmeyer, K.; Etzbach, K. H.; Ringsdorf, H.; Haarer, D. *Nature* **1994**, *371*, 141–143; (b) van de Craats, A. M.; de Haas, M. P.; Warman, J. M. *Synth. Met.* **1997**, *86*, 2125–2126; (c) van de Craats, A. M.; Warman, J. M.; Hasebe, H.; Naito, R.; Ohta, K. *J. Phys. Chem. B* **1997**, *101*, 9224–9232; (d) van de Craats, A. M.; Warman, J. M.; Müllen, K.; Geerts, Y.; Brand, J. D. *Adv. Mater.* **1998**, *10*, 36–38.
4. Ohta, K. *Ekisho* **2002**, *6*, 13–21.
5. Pisula, W.; Tomović, Ž.; Hamaoui, B. E.; Watson, M. D.; Pakula, T.; Müllen, K. *Adv. Funct. Mater.* **2005**, *15*, 893–904.
6. (a) Monobe, H.; Awazu, K.; Shimiz, Y. *Adv. Mater.* **2000**, *12*, 1495–1499; (b) Monobe, H.; Awazu, K.; Shimizu, Y. *Adv. Mater.* **2006**, *18*, 607–610; (c) Monobe, H.; Hori, H.; Shimizu, Y. *Mol. Cryst. Liq. Cryst.* **2007**, *475*, 13–22.
7. Terasawa, N.; Monobe, H.; Kiyohara, K.; Shimizu, Y. *Chem. Commun.* **2003**, 1678–1679.
8. (a) Hatsusaka, K.; Ohta, K.; Yamamoto, I.; Shirai, H. *J. Mater. Chem.* **2001**, *11*, 423–433; (b) Hatsusaka, K.; Kimura, M.; Ohta, K. *Bull. Chem. Soc. Jpn.* **2003**, *76*, 781–787; (c) Nekelson, F.; Monobe, H.; Shimizu, Y. *Mol. Cryst. Liq. Cryst.* **2007**, *479*, 205–211.
9. (a) Zeller, K.-P. *Azulene*; Houben-Weyl; Methoden der Organischen Chemie, 4th ed.; Georg Thieme: Stuttgart, Germany, 1985; Vol. V, Part 2c, pp 127–418; (b) Lemal, D. M.; Goldman, G. D. J. *J. Chem. Educ.* **1988**, *65*, 923–925.
10. (a) Praefcke, K.; Schmidt, D. *Z. Naturforsch., B: Anorg. Chem., Org. Chem.* **1981**, *36B*, 375–378; (b) Brettle, R.; Dunmur, D. A.; Estdale, S.; Marson, C. M. *J. Mater. Chem.* **1993**, *3*, 327–331; (c) Estdale, S. E.; Brettle, R.; Dunmur, D. A.; Marson, C. M. *J. Mater. Chem.* **1997**, *7*, 391–401; (d) Morita, T.; Takase, K.; Kaneko, M. Jpn. Patent 69436, 1990; (e) Morita, T.; Takase, K. Jpn. Patent 69437, 1990; (f) Morita, T.; Takase, K. Jpn. Patent 69438, 1990; (g) Morita, T.; Takase, K.; Kaneko, M. Jpn. Patent 69439, 1990; (h) Morita, T.; Takase, K.; Kaneko, M. Jpn. Patent 69441, 1990; (i) Morita, T.; Kaneko, M. Jpn. Patent 261753, 1991; (j) Morita, T.; Kaneko, M. Jpn. Patent 261754, 1991.
11. Ito, S.; Inabe, H.; Morita, N.; Ohta, K.; Kitamura, T.; Imafuku, K. *J. Am. Chem. Soc.* **2003**, *125*, 1669–1680.
12. Ito, S.; Ando, M.; Nomura, A.; Morita, N.; Kabuto, C.; Mukai, H.; Ohta, K.; Kawakami, J.; Yoshizawa, A.; Tajiri, A. *J. Org. Chem.* **2005**, *70*, 3939–3949.
13. Warman, J. M.; van de Craats, A. M. *Adv. Mater.* **2001**, *13*, 130–133.
14. Nozoe, T.; Asao, T.; Oda, M. *Bull. Chem. Soc. Jpn.* **1974**, *47*, 681–686.
15. Casado, J.; Ortiz, R. P.; Navarrete, J. T. L.; Ito, S.; Morita, N. *J. Phys. Chem. B* **2004**, *108*, 18463–18471.
16. Nguyen, H. T.; Destrade, C. *Mol. Cryst. Liq. Cryst.* **1984**, *92*, 257–262.
17. Pisula, W.; Kastler, M.; Wasserfallen, D.; Pakula, T.; Müllen, K. *J. Am. Chem. Soc.* **2004**, *126*, 8074–8075.
18. Schmidt-Mende, L.; Fechtenkötter, A.; Müllen, K.; Moons, E.; Friend, R. H.; MacKenzie, J. D. *Science* **2001**, *293*, 1119–1122.